Neural correlates of model-based and model-free reinforcement learning in Internet gaming disorder

Hangnyoung Choi

The Graduate School
Yonsei University
Department of Medicine

Neural correlates of model-based and model-free reinforcement learning in Internet gaming disorder

A Dissertation Submitted
to the Department of Medicine
and the Graduate School of Yonsei University
in partial fulfillment of the
requirements for the degree of
Doctor of Philosophy in Medical Science

Hangnyoung Choi

December 2024

This certifies that the Dissertation
of Hangnyoung Choi is approved.

Thesis Supervisor	Young-Chul Jung
Thesis Committee Member	Suk Kyoon An
Thesis Committee Member	Keun-Ah Choen
Thesis Committee Member	Jinna Kim
Thesis Committee Member	Woo-Young Ahn

The Graduate School
Yonsei University
December 2024

TABLE OF CONTENTS

LIST OF FIGURES

LIST OF TABLES

ABSTRACT

Neural correlates of model-based and model-free reinforcement learning in Internet gaming disorder

Background: Internet gaming disorder (IGD) has become a serious public health problem, but its neurocognitive mechanisms are unclear yet. Therefore, it is a crucial issue to identify similarities and differences between IGD and other addictive disorders including alcohol use disorder (AUD). Recent studies have supported that a computational psychiatric approach and decision-making framework might be advantageous in conceptualizing IGD and delineating its similarities and differences between psychiatric disorders. This study compared the neurocognitive features associated with model-based and model-free systems in individuals IGD and AUD.

Methods: Individuals diagnosed as IGD (n=24), AUD (n=22), and healthy controls (HC; n=30) in young males were scanned with fMRI while performing the two-step task, a well-validated task for appraising the contribution from two decision-making systems, goal-directed (model-based) and habitual (model-free) control systems. Goal of the present study is to investigate the balance between two decision-making systems (model-based/model-free learning) in IGD, AUD, and HC groups using computational modeling and hierarchical Bayesian analysis. Finally, we will describe neural correlates of goal-directed control of IGD and AUD via model-based fMRI analysis.

Results: The computational modeling results indicated that both the IGD and AUD groups exhibited similar levels of model-based behavior. However, there were notable differences in the neural correlates of the model-based reward prediction error (RPE) between the two groups. Specifically, the IGD group showed insula-specific activation linked to model-based RPE, whereas the AUD group displayed activation in the prefrontal regions, particularly the orbitofrontal cortex and superior frontal gyrus. Additionally, individuals with IGD demonstrated hyper-connectivity between the insula and other regions within the salience network in the context of model-based RPE.

Conclusions: The findings indicate that there may be distinct neurobiological mechanisms driving

model-based behavior in IGD and AUD, despite some shared cognitive features identified through computational modeling. As the inaugural neuroimaging study to compare IGD and AUD concerning the model-based system, this research offers new perspectives on the unique decision-making processes associated with IGD.

Clinical Relevance: This study highlights critical distinctions in the neurobiological mechanisms of decision-making processes between IGD and AUD. Understanding these differences is crucial for developing targeted therapeutic strategies. The identification of insula-specific activation in IGD and prefrontal activation in AUD suggests that interventions could be tailored to address these distinct neural pathways. For IGD, treatments focusing on modulating insula activity and enhancing salience network connectivity might prove effective. In contrast, AUD interventions might benefit from strategies aimed at improving prefrontal cortex function. These insights pave the way for personalized treatment approaches, potentially improving outcomes for individuals with IGD and AUD. Additionally, this research underscores the value of computational psychiatric approaches and neuroimaging in refining diagnostic criteria and therapeutic targets for addictive disorders.

Key words : Internet gaming disorder, alcohol use disorder, goal-directed control, model-based fMRI

1. Introduction

Internet gaming disorder (IGD) is defined as a maladaptive pattern of gaming behavior marked by diminished control and a heightened focus on gaming, often at the expense of occupational, social, and academic functioning. Research has consistently shown that IGD shares several cognitive, neural, and clinical characteristics with substance use disorders (SUD) and gambling disorder [1]. In 2018, the World Health Organization formally recognized gaming disorder as a medical condition in the International Classification of Diseases-11. Despite this recognition, ongoing debates persist regarding the classification of IGD as an addictive disorder alongside SUD[2–4]. Clinical distinctions between IGD and SUD have been noted, such as the lack of pharmacological effects leading to prominent physiological withdrawal and tolerance in IGD[5,6]. Consequently, further research is needed to elucidate the neurobiological underpinnings of IGD in comparison to substance-related addictive disorders.

The reinforcement learning model of addiction conceptualizes addiction as a progression from goal-directed actions to habitual, stimulus-driven behaviors[7,8]. Goal-directed actions rely on the "model-based" system, where potential actions are evaluated by anticipating their outcomes[9,10]. Conversely, habitual behaviors are governed by the "model-free" system, which depends on previously formed associations between stimuli and rewards[9,11]. While model-free decision-making is typically faster and more efficient, it tends to lack flexibility. Optimal decision-making involves a dynamic interplay between the model-based and model-free systems[12,13], but numerous studies indicate a disruption in the model-based system and a predominance of the model-free system in individuals with addiction[14–16]. For instance, individuals with alcohol use disorder (AUD) and binge drinkers show deficits in model-based control[17–21], with the severity of alcohol addiction inversely correlated with model-based behaviors in the general population[22]. Similarly, those with gambling disorder—a behavioral addiction not confounded by substance neurotoxicity—also exhibit impairments in model-based control[23].

To disentangle the contributions of model-based and model-free systems in decision-making, paradigms such as the two-stage task have been employed[24]. Early studies using this task in AUD populations revealed impaired model-based control, particularly after non-rewarded trials. In the general population, higher AUDIT scores correlated with reduced model-based control. While some studies found no impairments in model-based control among AUD individuals[19,25,26], those at high familial risk for AUD[27], or young social drinkers[28], growing evidence suggests that deficits in goal-directed control in AUD are linked to impaired model-based control. Sebold et al. (2017) reported that although reduced model-based control did not predict relapse in detoxified AUD individuals, high alcohol expectancies were negatively associated with model-based control in individuals with relapse, as shown by model-based fMRI analysis[21]. Furthermore, Chen et al. (2021) demonstrated a longitudinal link between impaired model-based control and higher binge

drinking trajectories in a large sample[17] . Interestingly, individuals with gambling disorder also exhibited impaired model-based control after unrewarded outcomes, a pattern similar to AUD, suggesting that this impairment may represent a shared feature of substance-related and behavioral addictions[23] . Despite extensive research on IGD, model-based system approaches have yet to be examined.

In this study, we aimed to investigate the balance between model-based and model-free systems in individuals with IGD and AUD using a two-stage task and model-based fMRI analysis. Model-based fMRI leverages the spatial and temporal resolution of task-based fMRI to capture neural activity associated with specific computational processes, distinguishing between competing models of neural and cognitive functions[29] . Key regions implicated in reward prediction, such as the ventromedial prefrontal cortex and ventral striatum, are thought to mediate model-based and model-free control.[13,24] This study seeks to compare the neural correlates of prediction error processing in IGD and AUD. We hypothesize that (1) individuals with IGD and AUD will exhibit impaired model-based control compared to healthy controls, and (2) the neural correlates of impaired model-based control will differ between IGD and AUD, reflecting the absence of alcohol-related neurotoxic effects in IGD.

2. MATERIALS AND METHODS

2.1. Participants

Seventy-seven male participants, aged 20 to 28, were recruited between September 2018 and August 2019 through community and university-based advertisements in Seoul, South Korea. During initial screening, participants were classified into the presumptive IGD group, AUD group, or healthy control (HC) group based on their scores from the Young Internet Addiction Test (IAT) and the Korean version of the Alcohol Use Disorder Identification Test (AUDIT). Subsequently, all participants underwent evaluation at Severance Hospital, where a board-certified psychiatrist conducted a semi-structured interview using the Structured Clinical Interview for the DSM-IV to assess for major psychiatric disorders. Based on DSM-5 diagnostic criteria, two psychiatrists reclassified participants into four groups: IGD, AUD, HC, or a comorbid group (IGD and AUD). Cognitive ability was assessed using the Korean version of the Wechsler Adult Intelligence Scale (K-WAIS-IV), and individuals with a verbal or performance IQ below 80 were excluded. Participants who were unable to undergo magnetic resonance imaging (MRI) were also excluded. To focus on the distinct pathologies of IGD and AUD, individuals with comorbid IGD and AUD were excluded. Additionally, participants with major psychiatric disorders, ongoing psychopharmacological treatment, or neurological conditions were excluded. After these criteria were applied, 74 participants remained for behavioral analysis and computational modeling.

For fMRI analysis, participants with an average framewise displacement exceeding 0.5 (N = 4) were excluded to ensure data quality. An additional participant was removed due to signal loss in frontal brain regions. This resulted in 69 participants being included in the fMRI analysis, divided into the following groups: HC (28), IGD (20), and AUD (21) (**Figure 1**). All participants provided detailed informed consent after receiving comprehensive information about the study protocol. The study was conducted in accordance with the ethical guidelines approved by the Institutional Review Board (IRB) of Severance Hospital, Seoul, South Korea (IRB approval number: 4-2014-0745).

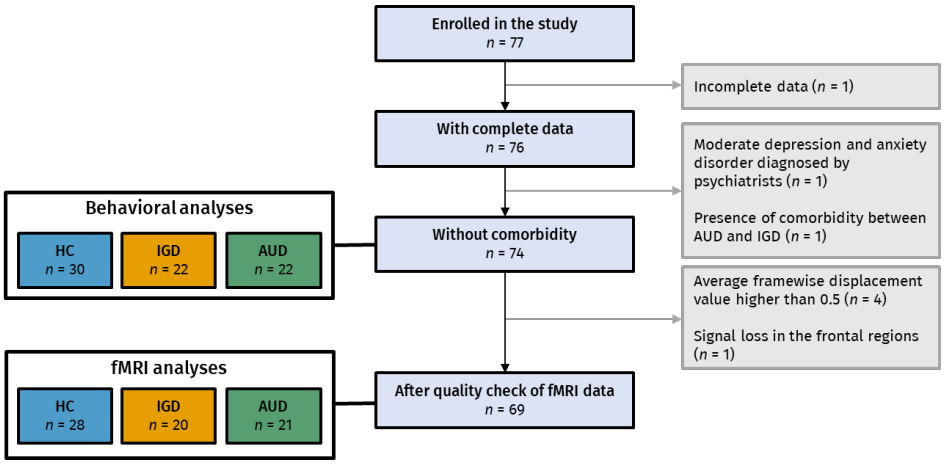

Figure 1. **Participant recruitment and inclusion process**[30]

2.2. Psychometric measure

Game and alcohol use were assessed using modified versions of the Internet Addiction Test (IAT)[31] and the Alcohol Use Disorder Identification Test (AUDIT)[32] , respectively. To measure the severity of depressive and anxiety symptoms, all participants completed the Beck Depression Inventory (BDI)[33] and the Beck Anxiety Inventory (BAI)[34] . Impulsivity was evaluated using the Barratt Impulsiveness Scale (BIS)[35] , while childhood symptoms of attention-deficit hyperactivity disorder (ADHD) were assessed with the Wender Utah Rating Scale (WURS)[36] . Group differences in survey measures were analyzed using a one-way analysis of variance (ANOVA) with group as the factor (IGD, AUD, HC). Post-hoc pairwise comparisons were conducted using Tukey's test.

2.3. fMRI data acquisition and preprocessing

MRI scanning was performed using a 3.0T MRI scanner (MagnetomVerio, Siemens Medical Solutions, Erlangen, Germany). Functional images were acquired with three 8.5-minutes runs using a T2*-weighted gradient echo-planar imaging sequence (30 axial slices, 4 mm thickness with 1 mm interslice gap; repetition time = 2,000 ms, echo time = 30 ms; flip angle = 90°; in-plane matrix size = 64 × 64 pixels; and field of view = 240 mm) while participants performed the two-stage task. Additionally, a structural T1-weighted gradient echo image was acquired (matrix size = 256 × 256, number of slices = 176, slice thickness = 1 mm, echo time = 2.46 ms, repetition time = 1,900 ms, field of view = 250 mm, flip angle = 9°, bandwidth = 170Hz/Px). Preprocessing of the fMRI data was conducted using fMRIPrep version 20.2.1. This included spatial normalization, susceptibility distortion correction, co-registration, and slice timing correction using fMRIPrep[37] .

2.4. Experimental task and procedure

Each participant completed 201 trials of the two-stage task, divided into three sessions (7.5 seconds per trial, approximately 8.38 minutes per session)[19] . In this task, a purely model-based learning agent is expected to alter their Stage 1 choice in the following trial if rewarded through an uncommon pathway. In contrast, a purely model-free learning agent, which does not account for the sequential structure of the task, would repeat the previous Stage 1 choice regardless of whether the reward was obtained through a common or uncommon pathway (**Figure 2**)[24] . Behavioral analysis measured the outcomes of Stage 1 and Stage 2 choices, state transitions, and whether participants received rewards on each trial. The task was implemented using E-Prime 3.0 software (**Figure 3**) (E-Prime Psychology Software Tools Inc., Pittsburgh, USA).

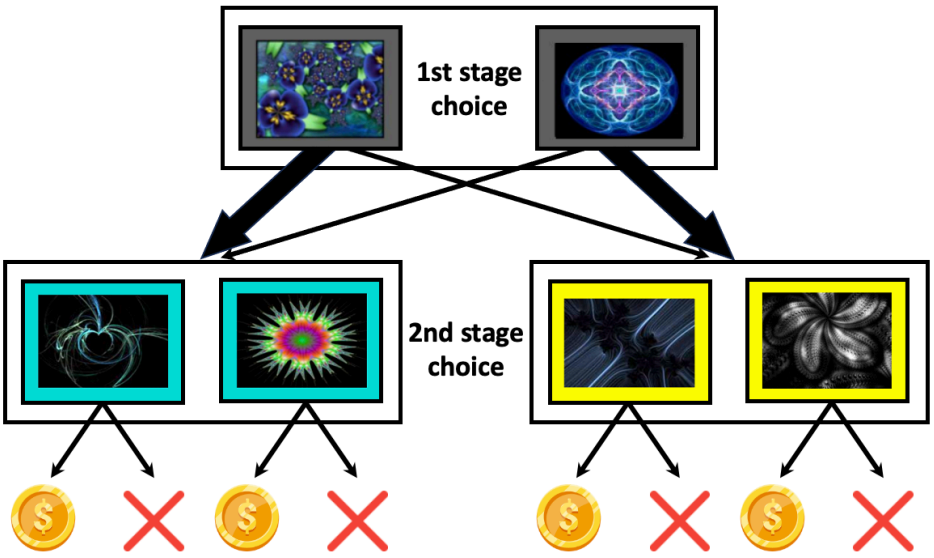

Figure 2. **Schematic representation of the two-stage task**[30] **.**

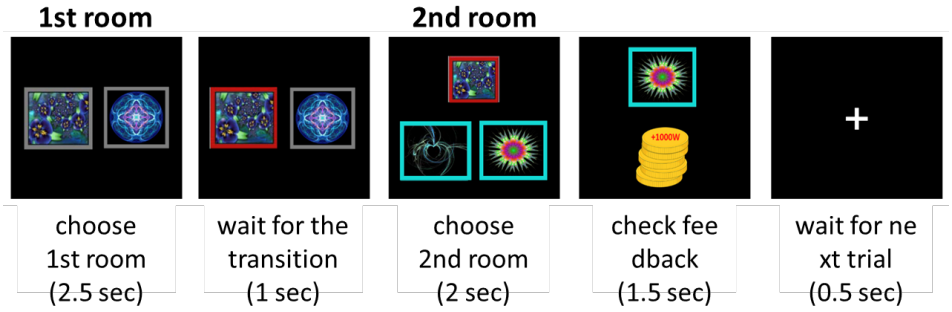

Figure 3. **Process of single task trial with time points.** Inside the fMRI scanner, participants completed 201 task trials, divided into three runs (7.5 seconds per trial, 8.38 minutes per run)[30] .

Before starting the task, participants were introduced to the storyline "treasure hunt in the color room" to help them grasp the sequential structure of the two-stage task as clearly as possible (**Figure S1).** A brief quiz was administered to confirm their understanding of the task. Following this, participants completed extensive practice sessions lasting up to 20 minutes. These practice tasks separated the Stage 1 choice task and the Stage 2 choice task, allowing participants to familiarize themselves with Stage 1 transitions and Stage 2 reward acquisition. The practice tasks used different fractal images than those in the actual two-stage task.

In the first stage, participants chose between two stimuli, with thick arrows (**Figure 2**) representing common transitions (70%) and thin arrows representing rare transitions (30%). For example,

selecting the left option in Stage 1 had a 70% probability of leading to the blue room in Stage 2 and a 30% probability of leading to the yellow room, with the probabilities reversed for the right option. In Stage 2, participants chose between two options, and rewards were determined by slowly fluctuating probabilities ranging from 0.25 to 0.75. Four distinct reward probability distributions were counterbalanced across groups. During the feedback stage, the selected stimulus from Stage 2 remained visible on the screen, and the outcome was displayed as either an image of coins labeled "+1000 W" (indicating a reward) or a red "X" (indicating no reward). The value of 1000 Korean won is approximately 0.76 USD.

A hypothetical model-based participant bases their choices on the task structure and transition probabilities. For instance, if a choice in Stage 1 leads to a reward through a common transition (70%), the model-based agent repeats the same choice in the next trial. However, if the reward is obtained via a rare transition (30%), the agent changes their choice. In contrast, a model-free participant relies solely on the outcome of the previous trial, repeating the same choice if rewarded and switching to the other option if not, regardless of the transition probabilities.

2.5. Statistical analyses

To analyze choice behavior, we employed a computational model based on the hybrid algorithm developed by Gläscher, Daw, Dayan, and O'Doherty (2010)[38] , as described by Daw et al. (2011)[24] . This hybrid model combines model-based reinforcement learning and model-free temporal difference learning. The model includes several key parameters: the model-based weight parameter (ω), which indicates the degree to which model-based learning influences behavior; the learning rate parameter (α), which measures how quickly expected values are updated based on reward prediction errors (RPEs), with higher values of α indicating faster updates; and the perseverance parameter (π), which reflects the propensity to repeat a previous choice regardless of expected value, with higher π values signifying stronger perseverance.

For each trial, we computed model-free and model-based RPEs, which represent the discrepancy between the reward received and the expected reward. Model parameters were estimated and compared across groups using hierarchical Bayesian analysis. To replicate a factorial analysis of choice behavior conducted by Daw, Gershman, Seymour, Dayan, and Dolan (2011)[24] , we calculated the stay probabilities for first-stage choices at the population level for each group. This stay probability represents the likelihood of selecting the same option as in the prior trial.

Additionally, we applied mixed-effects logistic regression to evaluate the impact of the preceding reward (whether the participant was rewarded in the previous trial), transition probability (whether the transition was common or rare), and their interaction on choice behavior. This analysis was conducted using the lme4 package in R[39] . The model included by-participant random intercepts and random slopes for the effects of reward and transition probability.

To further investigate individual behavior, we fitted each participant's trial-by-trial responses using the hybrid reinforcement learning model described in prior studies. This model assumes that choices are determined by a weighted combination of model-free and model-based learning processes, with the model-based weight parameter (ω) estimated for each participant. A value of ω = 1 corresponds to a purely model-based decision-making strategy.

$$V_{s1}^{Net} = \omega \cdot V_{s1}^{MB} + (1-\omega) \cdot V_{s1}^{MF}$$

The model-free algorithm, based on the temporal difference learning, updates the model-free value of each first-stage option, V_{s1}^{MF} by the reward prediction error (RPE) multiplied by a free first-stage learning rate parameter α_1 both at the onset of the second stage and reward outcome.

$$V_{s1}^{MF}(t+1) = V_{s1}^{MF}(t) + \alpha_1 \cdot (V_{s2,chosen}(t) - V_{s1}^{MF}(t))$$

$$V_{s1}^{MF}(t+1) = V_{s1}^{MF}(t) + \alpha_1 \cdot (reward - V_{s2}(t))$$

In contrast, the model-based algorithm computes the utility of each first-stage option by accounting for the transition structure.

$$V_{s1}^{MB} = p \cdot max(V_3, V_4) + (1-p) \cdot max(V_5, V_6),$$

In this task, the probability of a common transition is p=0.7, while the probability of a rare transition is p=0.3. The value of the second-stage options is updated exclusively through the model-free algorithm, as no further transitions occur after this stage, and only the reward outcome is provided. Consequently, the model-based and model-free values for the second-stage options are identical.

$$V_{s2}(t+1) = V_{s2}(t) + \alpha_2 \cdot (reward - V_{s2}(t))$$

The model applies the model-based and model-free values to a softmax function, which uses the free inverse temperature parameters for each stage (i.e., β_1, β_2) to quantify the stochasticity of each participant's choices. These parameters help estimate the probability of selecting each option. For instance, the probability of choosing option 2 in the first stage is calculated as follows:

$$P_2^{stage1} = \frac{1}{1 + exp(-\beta_1 \cdot (V_2^{Net} - V_1^{Net}) - \pi \cdot (C_1 - C_2))}$$

Here, V_2^{Net} and V_1^{Net} represent the net value of each first-stage option, calculated using Equation 1 mentioned earlier. The variable C_i equals 1 if the previous choice was option I; otherwise, C_i equals 0. The parameter π is a free perseverance parameter that reflects the participant's tendency to repeat the choice made in the previous trial. Overall, the model includes 6 parameters (α_1, α_2, β_1, β_2, π, ω).

We applied hierarchical Bayesian modeling to fit the model separately for each group. This approach incorporates group-level information about parameter values to inform individual-level parameter estimation, enhancing accuracy by regularizing individual variability in parameter estimates through shrinkage[40] . From this modeling, we extracted the group-level estimates for the six model parameters and compared them across groups (IGD vs. AUD, IGD vs. HC, and AUD vs. HC). To assess whether parameter estimates significantly differed between groups, we examined the 95% highest density interval (HDI) of the difference in parameter estimates (e.g., ω_IGD-ω_AUD). A significant difference was indicated if the 95% HDI did not include zero.

2.6. Model-based fMRI analyses

In the first-level analysis, we conducted a model-based fMRI analysis to identify voxels where blood oxygenation level-dependent (BOLD) activity correlated with model-free and model-based reward prediction errors (RPEs). Following the approach outlined by Daw et al. (2011)[24] , we first extracted time series of standard RPE estimates as the model-free regressor, aligning these with the onset of the second-stage transition and outcome delivery. For the model-based regressor, we computed a difference regressor by subtracting model-free RPE values from hypothetical RPE values that would occur if participants relied solely on a model-based strategy during the task. This difference regressor captures residual prediction error not explained by the model-free strategy and reflects model-based contributions. The model-based regressor was similarly derived at the second stage and outcome onset.

Additional regressors included the time points of choice responses in the first and second stages, as well as the onsets of fixation and the first stage, all with durations of 0.1 seconds. Six motion parameters estimated by fMRIPrep were incorporated as nuisance regressors to account for head movement. Using two parametric regressors of interest (model-free and model-based) and 10 nuisance regressors, we created two contrasts for each participant: one identifying voxels corresponding to model-free activity and the other to model-based activity.

In the second-level analysis, the first-level contrast images were subjected to a random effects analysis to produce group-level contrasts. Depression and anxiety scores were included as covariates to control the influence of psychiatric symptoms. Results were thresholded at $p<0.001$ (uncorrected for multiple comparisons) with an extent threshold of $k\geq10$ voxels. This threshold was selected to identify potentially meaningful neural activations across groups, given the exploratory nature of the study.

We also investigated correlations between neural activity showing significant group differences and the model-based weight parameter (ω). This analysis explored how the strength of neural correlates associated with model-based and model-free systems varied with the degree of model-based control. Mean beta values were extracted from peak voxels (within a 3 mm sphere) in each significant brain

region for each participant, and Pearson correlations were calculated with individual estimates of ω. This approach aimed to link model-based behavior with the corresponding neural correlates.

2.7. Functional connectivity analysis – Psychophysiological interaction analysis

In the model-based fMRI analysis, we identified the insula as a key region involved in model-based learning, particularly in the IGD group. To further explore how the insula interacts with other brain regions during model-based learning, we performed a psychophysiological interaction (PPI) analysis[41] . Given the role of the insular cortices as cortical hubs within the salience network[42,43] , we investigated the functional connectivity between the bilateral insula and other regions associated with this network.

In the first-level analysis, the left and right insula, defined as 3 mm spheres centered on the peak voxels identified in the second-level model-based fMRI analysis, were designated as seed regions. Model-free and model-based RPEs were included as parametric modulators, along with the four nuisance regressors and six motion regressors from the model-based fMRI analysis.

At the second level, we conducted one-sample t-tests within each group to examine connectivity patterns. Additionally, two-sample t-tests (HC vs. IGD, IGD vs. AUD, and HC vs. AUD) were performed to identify group differences. Depression and anxiety scores were included as covariates to control for the potential effects of psychiatric symptoms. The results were thresholded at $p < 0.001$ (uncorrected) with an extent threshold of $k \geq 10$ voxels. Small-volume correction was applied using a brain mask of the salience network to enhance specificity.

3. Results

3.1. Group difference in psychometric measures

To assess group differences in survey measures, we conducted a one-way analysis of variance (ANOVA) with group as the factor (i.e., IGD, AUD, HC) (Table 1), followed by post-hoc pairwise comparisons using Tukey's test (Figure 4). The IGD group exhibited the highest levels of internet addiction symptoms, while the AUD group showed the highest levels of alcohol use symptoms. Significant group differences were also observed in depression, anxiety, impulsivity, and childhood ADHD symptoms. Specifically, the IGD group reported greater depression symptoms compared to both the HC and AUD groups and higher anxiety symptoms than the HC group. Impulsivity scores were highest in the IGD group, followed by the AUD group and the HC group. Furthermore, the

IGD group reported the most pronounced childhood ADHD symptoms, with significant differences compared to both the HC and AUD groups. No significant group differences were found in IQ (including all subscales) or age.

Table 1 Demographics and clinical characteristics

	IGD	AUD	HC	F (p value)
Sample size	N = 22	N = 22	N = 30	
Age	23.73 (23.33, 24.13)	23.73 (23.18, 24.28)	22.6 (22.14, 23.06)	2.03 (p = 0.139)
Education	3.14 (2.95, 3.33)	3.32 (3, 3.64)	3.2 (2.98, 3.42)	0.13 (p = 0.882)
IAT	68 (66.34, 69.66)	32.05 (29.83, 34.26)	32.03 (29.67, 34.39)	84.72 (p < 0.001)
AUDIT	7.82 (5.96, 9.68)	24.36 (23.44, 25.29)	6.7 (5.86, 7.54)	62.58 (p < 0.001)
BDI	12.14 (10.52, 13.75)	7.45 (6.14, 8.77)	6.37 (5.3, 7.43)	5.36 (p < 0.05)
BAI	9.41 (7.98, 10.84)	7.45 (5.81, 9.1)	4.57 (3.73, 5.4)	3.91 (p < 0.05)
BIS	56.18 (54.06, 58.3)	50.05 (48.3, 51.79)	44.93 (43.57, 46.29)	11.21 (p < 0.001)
WURS	29.23 (26.62, 31.83)	19.55 (16.73, 22.36)	18.97 (16.71, 21.22)	4.91 (p < 0.05)
IQ (K-WAIS)	111.64 (109.07, 114.21)	112.45 (110.36, 114.55)	110.43 (108.24, 112.63)	0.21 (p = 0.814)
VCI	103.86 (101.27, 106.45)	104.09 (101.52, 106.66)	107.47 (104.97, 109.97)	0.67 (p = 0.516)
PRI	115.27 (112.38, 118.17)	109.05 (105.87, 112.22)	108.73 (106, 111.47)	1.50 (p = 0.23)

Data under the first three columns are the means (95% confidence interval) for each group (IGD, AUD, and HC) or numbers for sample size. Results of a one-way analysis of variance (ANOVA) with group factors (i.e., IGD, AUD, HC) are shown in the rightmost column; F-statistics and p-value. IAT, Young Internet Addiction Test; AUDIT, Alcohol Use Disorder Identification Test; BDI, Beck Depression Inventory; BAI, Beck Anxiety Inventory; BIS, Barratt Impulsiveness Scale; WURS, Wender Utah Rating Scale; K-WAIS, the Korean version of the Wechsler Adult Intelligence Scale; VCI, Verbal Comprehension Index Scale; PRI, Perceptual Reasoning Index Scale[30] .

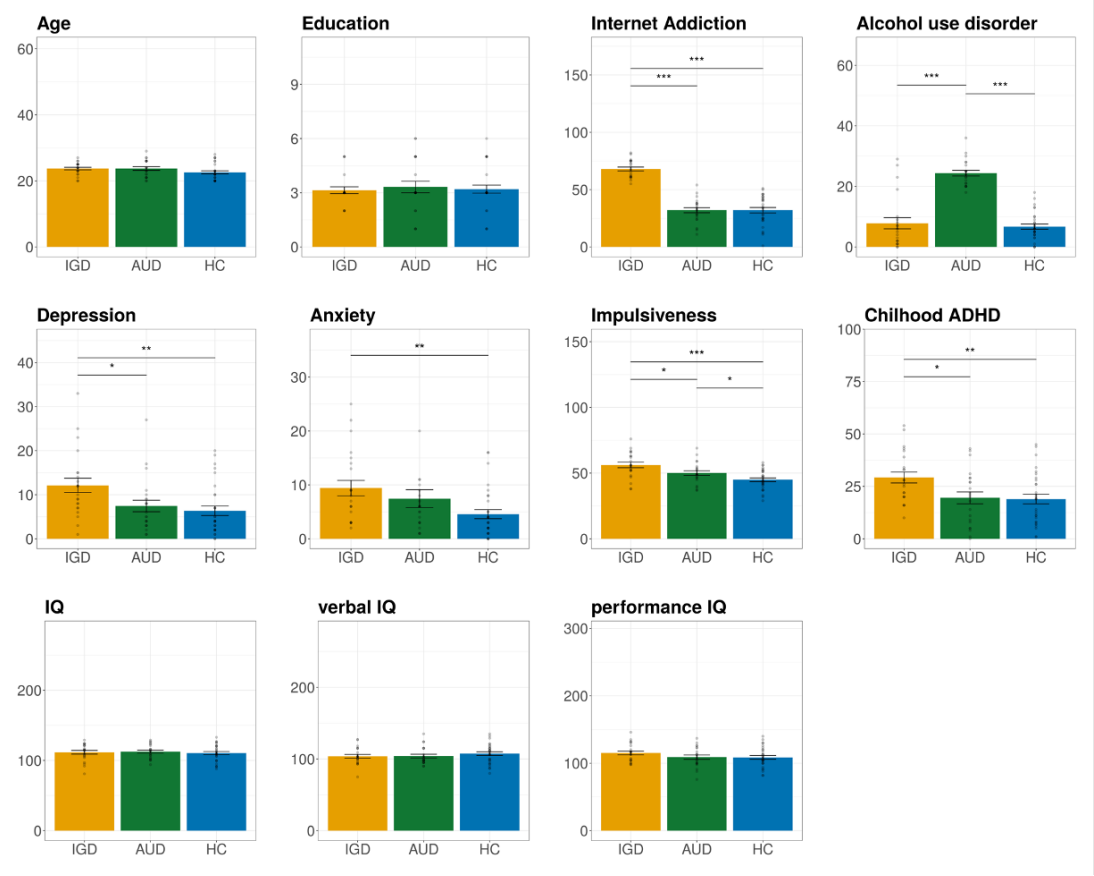

Figure 4. Group differences in psychometric measures. Each bar indicates the means of each group. Error bars are 95% confidence interval, and dots correspond to each participant's data. Measures with significant group differences are flagged with asterisks (*, $p < 0.05$; **, $p < 0.005$; ***, $p < 0.001$)[30] .

3.2. Behavioral results

The observed stay probability (**Figure 5**) shows a combination of model-based and model-free learning in all three groups, which were also supported by the mixed effects logistic regression results. The main effect of reward (IGD, B=-1.117, 95% confidence interval (CI)=[-1.440, -0.794], p=1.19e-11; AUD, B=-1.119, 95% CI=[-1.536, -0.702], p=1.44e-07; HC, B=-0.778, 95% CI=[-1.129, -0.427], p=1.40e-05) and transition probability (IGD, B=-1.055, 95% CI=[-1.374, -0.735], p=9.38e-11; AUD, B=-1.238, 95% CI=[-1.954, -0.523], p=0.001; HC, B=-1.077, 95% CI=[-1.406, -0.748], p=1.40e-10) were significant in all three groups, indicating that all groups accounted for

both rewards (i.e., model-free learning) and the transition structure (i.e., model-based learning) when making choices (**Table S1**). The combination of model-based and model-free strategy was also supported by significant main effect of interaction between reward and transition probability (IGD, B=3.311, 95% CI=[2.912, 3.709], p<2.00e-16; AUD, B=3.204, 95% CI=[-2.776, 3.631], p<2.00e-16; HC, B=1.970, 95% CI=[1.661, 2.279], p<2.00e-16).

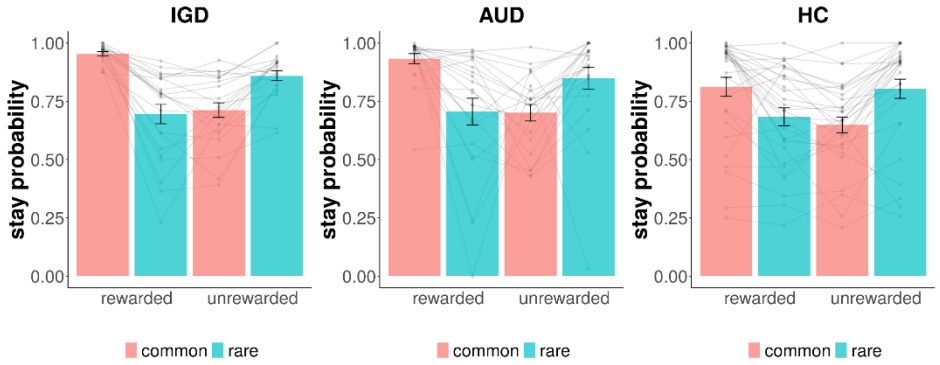

Figure 5. **Stay probability by group.** The observed stay proportions for each group are shown as a function of reward and transition probability. Each dot represents individual participant data, connected by lines. Error bars indicate the standard error of the mean (SEM)[30] .

3.3. Model comparison

We evaluated three models: a seven-parameter model from Daw, Gershman, Seymour, Dayan, and Dolan (2011), a six-parameter model, and a four-parameter model. Each model was fitted separately for each group (IGD, AUD, HC) using hierarchical Bayesian modeling. To assess model fit, we calculated the leave-one-out information criterion (LOOIC) using the "loo" package in R. **Table 2** presents the LOOIC values for each model across the groups. As a lower LOOIC indicates a better model fit, the six-parameter model provided the best fit for all three groups. Consequently, the six-parameter model was selected for further analyses.

Table 2. Model comparison results

	IGD	AUD	HC
Four-parameter model	7779.664	8104.869	11907.628
Six-parameter model	**7711.565**	**8062.970**	**11838.170**
Seven-parameter model	7715.729	8064.469	11840.879

The table shows the leave-one-out information criterion (LOOIC) for the seven-parameter, six-parameter, and four-parameter models across the IGD, AUD, and HC groups. The model with the lowest LOOIC value (indicating the best fit) for each group is highlighted in bold[30] .

3.4. Modelling results

We found significant group differences in the second-stage learning rate parameter α_2 and perseverance parameter π (**Figure 6**). AUD and IGD groups showed higher α_2 (α_(2,IGD)-α_(2,HC) 95% HDI = [0.072, 0.359]; α_(2,IGD)-α_(2,HC) 95% HDI = [0.011, 0.313]) and higher π estimates (π_IGD-π_HC 95% HDI = [0.1, 0.1.059]; π_AUD-π_HC 95% HDI = [00.01, 1.021]) compared to the HC group. There were no group differences in the model-based weight parameter ω, first-stage learning rate α_1, and first- and second-stage inverse temperature β_1 and β_2. See **Figure S2** for the distribution of group differences in the model parameter estimates.

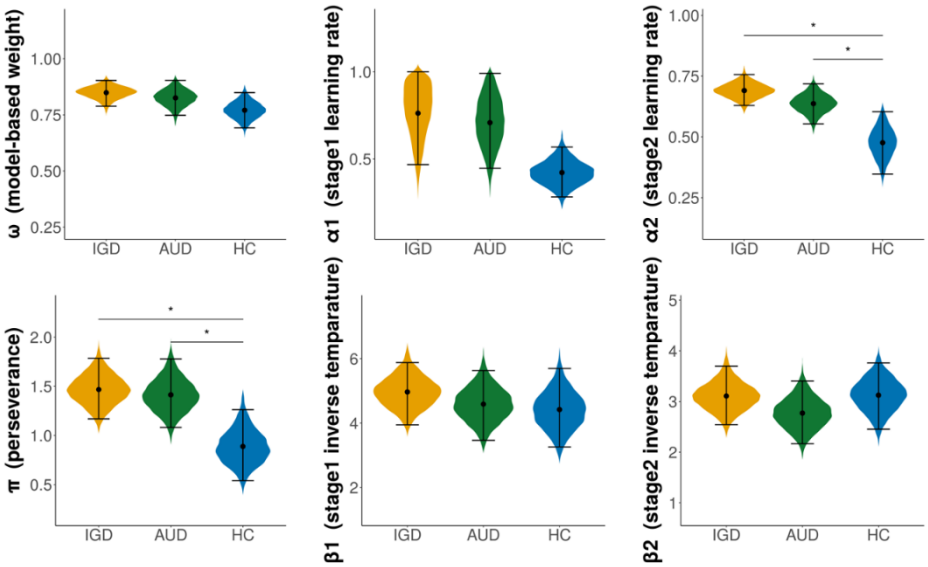

Figure 6. **Group comparison of parameter estimates.** Estimates of six model parameter value of each group (IGD, AUD, HC group). Error bars are 95% highest density interval (HDI). Model parameters with significant group differences are flagged with asterisks[30] .

3.5. Model-based fMRI results

The model-based fMRI analysis revealed significant differences among the HC, IGD, and AUD groups when the model-based RPE was used as a parametric modulator (**Figures 7A and 7B**). Specifically, the right orbitofrontal cortex (OFC) in the AUD group showed a stronger correlation

with the model-based RPE compared to the IGD group ($t=4.22$, $k=13$, $p<0.001$). In the IGD group, bilateral insular activation demonstrated a stronger correlation with the model-based RPE compared to the HC group (left: $t=4.20$, $k=17$, $p<0.001$; right: $t=4.71$, $k=33$, $p<0.001$). Furthermore, the left superior frontal gyrus (SFG) in the AUD group exhibited a stronger correlation with the model-based RPE compared to the HC group ($t=4.18$, $k=26$, $p<0.001$). No significant group differences were observed when the model-free RPE was used as a parametric modulator. Detailed second-level results for each group are presented in **Table S2**.

Further analysis explored the relationship between the significant findings of the model-based fMRI analysis (i.e., the correlation of each region with model-based RPE) and the level of model-based control, as indicated by individual estimates of ω. In the IGD group, a negative correlation was found between the beta value of the right insula and ω ($r=-0.45$, $p<0.05$), suggesting that individuals with lower model-based weight parameter estimates had stronger coupling between the right insula and the model-based RPE. This correlation was not observed in the AUD group ($r=-0.09$, $p=0.709$) or the HC group ($r=-0.19$, $p=0.334$) (**Figure 7C**). No significant correlations were identified for the left insula.

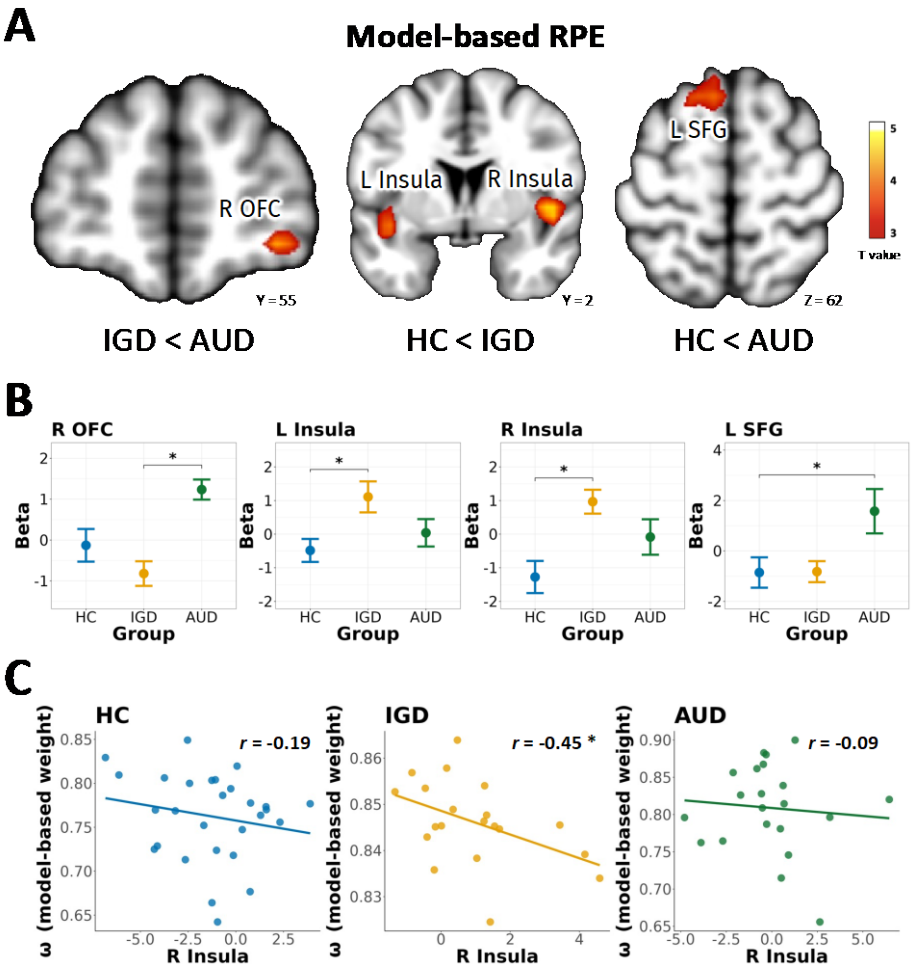

Figure 7. Differences in model-based fMRI analysis across groups. (A) Brain regions showing significant group differences identified through second-level two-sample comparisons, using model-based reward prediction error (RPE) as parametric modulators ($p < 0.001$, uncorrected; cluster size, $k \geq 10$). Significant differences indicate that one group's brain activation is more strongly correlated with the model-based RPE than another. The color bar represents t-statistics derived from the two-sample t-tests. (B) Group-wise average beta values extracted from 3mm spheres at peak MNI coordinates (R OFC: 35, 55, -8; L Insula: -40, 2, -8; R Insula, 46, 2, 2; L SFG: -6, 25, 62) for brain regions displaying significant group differences. Each dot corresponds to the group-wise mean beta value for each region, with error bars representing the standard error. Asterisks denote significance from two-sample t-test ($p < 0.001$). (C) Correlation between beta values in the left insula and the model-based weight parameter (ω) estimates. Each dot represents the beta value of the right insula (extracted from 3mm spheres at peak MNI coordinates: 46, 2, 2)

from the first-level analysis on the x-axis, and the individual estimates of the model-based weight parameter on the y-axis. The regression line illustrates the Pearson correlation between the beta value of the right insula and the ω estimates. A significant correlation ($p < 0.05$) is marked with an asterisk. OFC = orbitofrontal cortex; SFG = superior frontal gyrus[30] .

3.6. Psychophysiological interaction analysis results

The PPI analysis identified significant correlations between the insula and other brain regions within the salience network, specifically in the IGD group (**Figure 8** & **Table S3**). For model-based RPE, the right insula was correlated with the right putamen (t=5.23, p<0.001), left insula (t=5.75, p<0.001), and occipital lobe (t=4.23~4.37, p<0.001). Similarly, the left insula was correlated with the anterior cingulate cortex (ACC; t=4.24, p<0.001), right superior temporal gyrus (STG; t=3.67, p<0.001), and occipital lobe (t=3.72~5.14, p≤0.001). Group comparisons revealed distinctive connectivity patterns unique to IGD group (**Table S4**). The connectivity between the right insula and the left insula was greater in the IGD group compared to HC (t=3.89, p<0.001). Furthermore, connectivity between the insula and occipital lobe was greater in the IGD group compared to the AUD (right insula as seed: t=3.52~4.41, p<0.001; left insula as seed: t=3.52~3.57, p<0.001) and HC (left insula as seed: t=3.41~3.79, p<0.001). These findings highlight that IGD is characterized by distinctive patterns of hyper-connectivity involving the insula and its interactions with the salience network. This suggests a potential link between these unique connectivity patterns and ongoing reward processes specific to the IGD group during model-based learning.

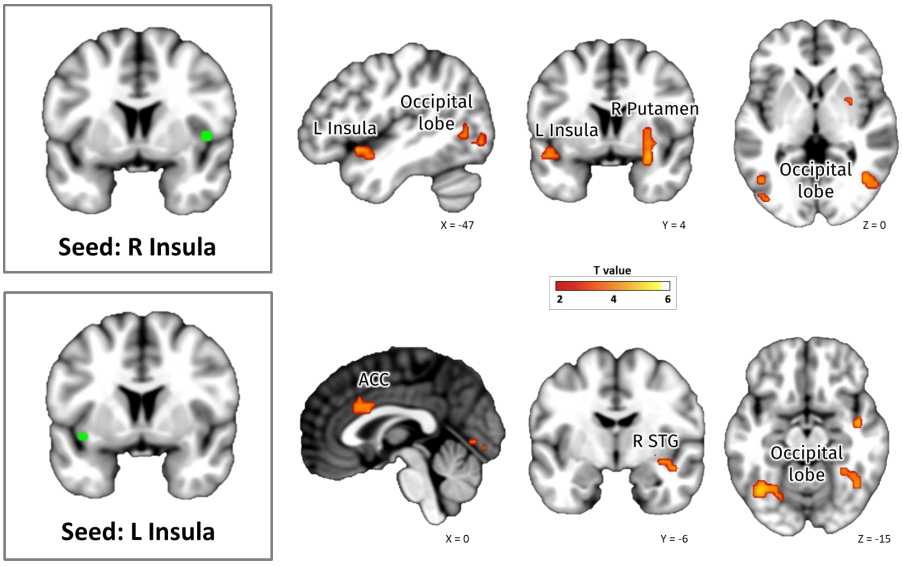

Figure 8. Psychophysiological interaction (PPI) analysis results for the internet gaming disorder group. Using the right insula (MNI-coordinates: -40, 2, -8) and left insula (MNI-coordinates: 46, 2, 2) as seed regions (3mm spheres), a PPI analysis employed model-based reward prediction error (RPE) as the psychological variable. The brain maps depict the effects of model-based RPE on each insula to the whole brain of the IGD group ($p < 0.001$, uncorrected; cluster size, $k \geq 10$)[30].

4. Discussion

In this study, we examined the neurocognitive features associated with model-based learning in individuals with Internet Gaming Disorder (IGD) and Alcohol Use Disorder (AUD). The primary findings are as follows:

1. Contrary to our initial hypothesis, both the IGD and AUD groups demonstrated higher learning rate and perseverance parameter estimates compared to the healthy control (HC) group.
2. The insula played a distinct role in processing model-based behavior specific to the IGD group. In IGD participants, model-based reward prediction error (RPE) was significantly correlated with bilateral insula activation, whereas in the AUD group, it correlated with activation in the frontal regions, specifically the right orbitofrontal cortex (OFC) and left superior frontal gyrus (SFG).
3. The IGD group uniquely exhibited hyper-connectivity between the bilateral insula and other regions of the salience network, including the putamen, anterior cingulate cortex (ACC), superior temporal gyrus (STG), and occipital lobe, in the context of model-based RPE.
4. Additionally, in the IGD group, the correlation between the right insula and model-based RPE was notably stronger in individuals exhibiting lower levels of model-based behavior (i.e., lower ω).

These findings highlight distinct neurobiological pathways for model-based learning in IGD and AUD, emphasizing the critical role of the insula in IGD.

The finding of similarly high levels of model-based behavior across all groups was consistently supported by behavioral and computational modeling analyses. While previous studies have reported mixed evidence of impaired model-based behavior in individuals with AUD[17–20,27,44],

recent research by Silva and Hare (2020)[45] suggests that humans tend to rely on model-based inference when they have a clear understanding of the task. In this study, we adopted several procedures recommended by Silva and Hare (2020)[45] to ensure participants comprehended the two-stage task. Additionally, participants exhibited above-average working memory and processing speed, surpassing values reported in prior research[46]. These enhanced cognitive abilities may have contributed to the observed preservation of model-based behavior in both IGD and AUD participants compared to healthy controls. However, these interpretations remain speculative and require further confirmation. Future research should include participants with a broader range of cognitive abilities and experimentally manipulate task understanding to validate and generalize these findings.

Although the degree of model-based control (i.e., ω) was comparable across groups, the IGD and AUD groups demonstrated elevated α_2 and π estimates, suggesting shared cognitive characteristics between alcohol and gaming addiction. Impulsivity, a well-established personality trait related to addiction[47–49], may underlie the higher learning rate (α_2) estimates, reflecting heightened reward sensitivity and reduced cognitive control. The tendency for addicted individuals to update immediate rewards more quickly could indicate either an increased salience of immediate rewards or a diminished capacity to suppress responses to them[50]. While a higher learning rate can be advantageous in rapidly changing or uncertain environments, it may pose challenges in contexts like the two-stage task, where reward probabilities shift more gradually[51]. This implies that individuals with IGD and AUD may find it difficult to adjust their learning strategies appropriately in situations requiring slower, more deliberate updates to reward expectations.

The elevated perseverance parameter (π) estimates observed in the IGD and AUD groups suggest a stronger tendency to repeat prior choices independent of reward outcomes, potentially reflecting habitual behavior or compulsivity—core features of addictive disorders[15,52,53]. This aligns with previous studies reporting increased perseverance in individuals with addiction, reinforcing the idea that heightened perseveration may represent a maladaptive trait associated with addiction[54,55]. The combined pattern of higher learning rates and greater perseverance seen in both groups may highlight shared neurocognitive characteristics underlying addictive behaviors. Nonetheless, additional research is required to confirm and further explore these findings.

Using fMRI, we identified distinct neural patterns associated with model-based behavior in the IGD group compared to the AUD group. Notably, our findings emphasize the unique involvement

of the insula in model-based behavior among individuals with IGD. The insula is a vital component of the brain's salience network[56,57] , which plays a key role in encoding prediction errors related to reward variability[58] and processing salient stimuli[42,59] . Previous research has shown hyper-connectivity of the salience network in individuals with behavioral addictions during resting states[60] , and in individuals with IGD specifically during resting states, risky decision-making, and executive control tasks[61–64] . Consistent with these findings, our results indicate that heightened sensitivity of the insula, a central hub of the salience network, may represent a distinct neural marker of IGD.

To interpret the hyperactivation of the insula observed specifically in the IGD group, it is crucial to examine its established role in drug craving and addiction[65] . Studies have shown that lesions in the insular cortex can disrupt addictive behaviors, emphasizing the insula's central role in addiction mechanisms[66] . However, neuroimaging studies on substance use disorders (SUDs) often report insula hypoactivation during decision-making tasks[67–69] . This apparent contradiction may arise from differences in the processing of drug-related versus non-drug-related rewards in individuals with addiction[70] . While drugs of addiction represent highly salient rewards and lead to hyperactivation of the salience network, non-drug rewards are typically associated with reduced activity in this network when compared to non-addicted individuals[71] . Thus, the insula hypoactivation reported in decision-making tasks for SUDs may be attributable to the use of non-salient rewards. Similarly, neuroimaging studies on IGD employing gaming-related cues have demonstrated increased activation of the salience network[72–74] . Given the task dynamics and reward structure in our study, which likely mirrors gaming behavior more closely than substance use, the pronounced insula activation observed in the IGD group may indicate that participants approached the two-stage task in a manner akin to playing a game.

Another noteworthy observation is the hyperactivation of prefrontal regions, specifically the OFC and SFG, in individuals with AUD during model-based behavior. The OFC plays a crucial role in regulating goal-directed, or model-based, action planning and execution[75–78] , encoding the value of stimuli, and understanding the relationship between stimuli and their expected outcomes[79,80] . Similarly, the SFG is involved in higher-order cognitive functions, including working memory and executive processing[81] . While previous studies have generally reported decreased prefrontal activation in individuals with AUD during decision-making tasks and at rest[82,83] , our study revealed increased activation in these regions. This discrepancy may be attributed to variations in

model-based performance, as we did not observe impairments in model-based control among individuals with AUD, unlike prior findings in AUD or other SUDs. These results corroborate previous research suggesting that compensatory hyperactivation in prefrontal regions may support task performance in AUD[84] . Extending this interpretation, the hyperactivation observed in the AUD group might represent a compensatory mechanism to counteract deficits in model-based systems, thereby facilitating model-based behavior. Notably, such compensatory hyperactivation in the frontal regions appears specific to AUD and is absent in IGD. This distinction might stem from the absence of chemical intoxication in IGD, which is a characteristic feature of AUD and other SUDs[85–88] .

To our knowledge, this is the first neuroimaging study to compare IGD and AUD with a focus on model-based behavior. The findings suggest that while IGD and AUD share cognitive features related to reward sensitivity and compulsivity, the underlying neural mechanisms differ. These differences may reflect variations in reward salience and distinct brain adaptations associated with alcohol and gaming behaviors. The study provides valuable insights into the neurocognitive mechanisms underlying addictive disorders and emphasizes the need for further research to investigate the roles of the insula and salience network in IGD.

Despite its contributions, this study has limitations. First, we used a fixed 0.5-second inter-trial interval without jittering, which may have resulted in overlapping blood oxygen level-dependent (BOLD) responses across trials[89] . Future studies should include jittered inter-trial intervals to address this issue. Second, as an initial study comparing neural correlates of model-based behavior in IGD and AUD, our statistical methods lacked specificity in distinguishing shared and unique neural correlates between groups. More precise approaches are required for future research. Finally, the generalizability of our findings is limited by the small sample size and the characteristics of the participants. Although participants were diagnosed with IGD or AUD by psychiatrists, they were recruited from community settings rather than clinical populations, potentially leading to differences in symptom severity. Additionally, the sample included only young men, and most participants in the IGD group primarily engaged in multiplayer online battle arena (MOBA) games, influenced by Korean cultural preferences. Future research should consider cultural contexts, use larger and more diverse samples, and apply stricter statistical thresholds.

5. Conclusion

This study provides novel insights into the neurocognitive features and neural correlates of model-based learning in individuals with IGD and AUD. While both groups exhibited similar levels of model-based behavior, their neural signatures differed were observed: the insula was uniquely involved in IGD, while prefrontal regions played a prominent role in AUD. These findings suggest potential differences in the neurobiological mechanisms underlying addictive behaviors in IGD and AUD, contributing to the growing body of evidence that highlights both shared and unique features of IGD and substance-related addictive disorders. Further research with larger samples and consideration of cultural influences is necessary to better understand the pathophysiology of IGD and refine its diagnostic and treatment approaches.

References

1. Vaccaro, A. G. & Potenza, M. N. Diagnostic and Classification Considerations Regarding Gaming Disorder: Neurocognitive and Neurobiological Features. *Front. Psychiatry* **10**, 405 (2019).

2. Kuss, D. J., Griffiths, M. D. & Pontes, H. M. Chaos and confusion in DSM-5 diagnosis of Internet Gaming Disorder: Issues, concerns, and recommendations for clarity in the field. *J. Behav. Addict.* **6**, 103–109 (2017).

3. Saunders, J. B. *et al.* Gaming disorder: Its delineation as an important condition for diagnosis, management, and prevention. *J. Behav. Addict.* **6**, 271–279 (2017).

4. Starcevic, V. Internet gaming disorder: Inadequate diagnostic criteria wrapped in a constraining conceptual model. *J. Behav. Addict.* **6**, 110–113 (2017).

5. King, D. L., Herd, M. C. E. & Delfabbro, P. H. Tolerance in Internet gaming disorder: A need for increasing gaming time or something else? *J. Behav. Addict.* **6**, 525–533 (2017).

6. Yen, J.-Y., Lin, P.-C., Wu, H.-C. & Ko, C.-H. The withdrawal-related affective, gaming urge, and anhedonia symptoms of internet gaming disorder during abstinence. *J. Behav. Addict.* **11**, 481–491 (2022).

7. Everitt, B. J. & Robbins, T. W. Neural systems of reinforcement for drug addiction: from actions to habits to compulsion. *Nat. Neurosci.* **8**, 1481–1489 (2005).

8. Lüscher, C., Robbins, T. W. & Everitt, B. J. The transition to compulsion in addiction. *Nat. Rev. Neurosci.* **21**, 247–263 (2020).

9. Daw, N. D., Niv, Y. & Dayan, P. Uncertainty-based competition between prefrontal and dorsolateral striatal systems for behavioral control. *Nat. Neurosci.* **8**, 1704–1711 (2005).

10. Dayan, P. & Niv, Y. Reinforcement learning: The Good, The Bad and The Ugly. *Curr. Opin. Neurobiol.* **18**, 185–196 (2008).

11. Schultz, W., Dayan, P. & Montague, P. R. A Neural Substrate of Prediction and Reward. *Science* **275**, 1593–1599 (1997).

12. Drummond, N. & Niv, Y. Model-based decision making and model-free learning. *Curr. Biol.* **30**, R860–R865 (2020).

13. Lee, S. W., Shimojo, S. & O'Doherty, J. P. Neural Computations Underlying Arbitration between Model-Based and Model-free Learning. *Neuron* **81**, 687–699 (2014).

14. Groman, S. M., Massi, B., Mathias, S. R., Lee, D. & Taylor, J. R. Model-Free and Model-Based Influences in Addiction-Related Behaviors. *Biol. Psychiatry* **85**, 936–945 (2019).

15. Lucantonio, F., Caprioli, D. & Schoenbaum, G. Transition from 'model-based' to 'model-free' behavioral control in addiction: Involvement of the orbitofrontal cortex and dorsolateral striatum. *Neuropharmacology* **76**, 407–415 (2014).

16. Voon, V., Reiter, A., Sebold, M. & Groman, S. Model-Based Control in Dimensional Psychiatry. *Biol. Psychiatry* **82**, 391–400 (2017).

17. Chen, H. *et al.* Model-Based and Model-Free Control Predicts Alcohol Consumption Developmental Trajectory in Young Adults: A 3-Year Prospective Study. *Biol. Psychiatry* **89**, 980–989 (2021).

18. Doñamayor, N., Strelchuk, D., Baek, K., Banca, P. & Voon, V. The involuntary nature of binge drinking: goal directedness and awareness of intention. *Addict. Biol.* **23**, 515–526 (2018).

19. Voon, V. *et al.* Disorders of compulsivity: a common bias towards learning habits. *Mol. Psychiatry* **20**, 345–352 (2015).

20. Sebold, M. *et al.* Model-Based and Model-Free Decisions in Alcohol Dependence. *Neuropsychobiology* **70**, 122–131 (2014).

21. Sebold, M. *et al.* When Habits Are Dangerous: Alcohol Expectancies and Habitual Decision Making Predict Relapse in Alcohol Dependence. *Biol. Psychiatry* **82**, 847–856 (2017).

22. Gillan, C. M., Kosinski, M., Whelan, R., Phelps, E. A. & Daw, N. D. Characterizing a psychiatric symptom dimension related to deficits in goal-directed control. *eLife* **5**, e11305 (2016).

23. Wyckmans, F. *et al.* Reduced model-based decision-making in gambling disorder. *Sci. Rep.* **9**, 19625 (2019).

24. Daw, N. D., Gershman, S. J., Seymour, B., Dayan, P. & Dolan, R. J. Model-Based Influences on Humans' Choices and Striatal Prediction Errors. *Neuron* **69**, 1204–1215 (2011).

25. Hogarth, L. *et al.* Intact goal-directed control in treatment-seeking drug users indexed by outcome-devaluation and Pavlovian to instrumental transfer: critique of habit theory. *Eur. J. Neurosci.* **50**, 2513–2525 (2019).

26. Deserno, L. *et al.* Lateral prefrontal model-based signatures are reduced in healthy individuals with high trait impulsivity. *Transl. Psychiatry* **5**, e659–e659 (2015).

27. Reiter, A. M. F., Deserno, L., Wilbertz, T., Heinze, H.-J. & Schlagenhauf, F. Risk Factors for Addiction and Their Association with Model-Based Behavioral Control. *Front. Behav. Neurosci.* **10**, 26 (2016).

28. Nebe, S. *et al.* No association of goal-directed and habitual control with alcohol consumption in young adults. *Addict. Biol.* **23**, 379–393 (2018).

29. O'DOHERTY, J. P., HAMPTON, A. & KIM, H. Model-Based fMRI and Its Application to Reward Learning and Decision Making. *Ann. N. York Acad. Sci.* **1104**, 35–53 (2007).

30. Kwon, M., Choi, H., Park, H., Ahn, W.-Y. & Jung, Y.-C. Neural correlates of model-based behavior in internet gaming disorder and alcohol use disorder. *J. Behav. Addict.* **13**, 236–249 (2024).

31. YOUNG, K. S. Internet Addiction: The Emergence of a New Clinical Disorder. *CyberPsychology Behav.* **1**, 237–244 (1998).

32. SAUNDERS, J. B., AASLAND, O. G., BABOR, T. F., FUENTE, J. R. D. L. & GRANT, M. Development of the Alcohol Use Disorders Identification Test (AUDIT): WHO Collaborative Project on Early Detection of Persons with Harmful Alcohol Consumption-II. *Addiction* **88**, 791–804 (1993).

33. Beck, A. T., Steer, R. A., Ball, R. & Ranieri, W. F. Comparison of Beck Depression Inventories-IA and-II in Psychiatric Outpatients. *J. Pers. Assess.* **67**, 588–597 (1996).

34. Beck, A. T., Epstein, N., Brown, G. & Steer, R. A. An inventory for measuring clinical anxiety: Psychometric properties. *J. Consult. Clin. Psychol.* **56**, 893–897 (1988).

35. Patton, J. H., Stanford, M. S. & Barratt, E. S. Factor structure of the barratt impulsiveness scale. *J. Clin. Psychol.* **51**, 768–774 (1995).

36. Ward, M. F., Wender, P. H. & Reimherr, F. W. The Wender Utah Rating Scale: an aid in the retrospective diagnosis of childhood attention deficit hyperactivity disorder [published erratum appears in Am J Psychiatry 1993 Aug;150(8):1280]. *Am. J. Psychiatry* **150**, 885–890 (1993).

37. Esteban, O. *et al.* fMRIPrep: a robust preprocessing pipeline for functional MRI. *Nat. Methods* **16**, 111–116 (2019).

38. Gläscher, J., Daw, N., Dayan, P. & O'Doherty, J. P. States versus Rewards: Dissociable Neural Prediction Error Signals Underlying Model-Based and Model-Free Reinforcement Learning. *Neuron* **66**, 585–595 (2010).

39. Bates, D., Mächler, M., Bolker, B. & Walker, S. Fitting Linear Mixed-Effects Models Using lme4. *J. Stat. Softw.* **67**, (2015).

40. Ahn, W.-Y., Krawitz, A., Kim, W., Busemeyer, J. R. & Brown, J. W. A Model-Based fMRI Analysis With Hierarchical Bayesian Parameter Estimation. *J. Neurosci., Psychol., Econ.* **4**, 95–110 (2011).

41. Friston, K. J. *et al.* Psychophysiological and Modulatory Interactions in Neuroimaging. *NeuroImage* **6**, 218–229 (1997).

42. Seeley, W. W. *et al.* Dissociable Intrinsic Connectivity Networks for Salience Processing and Executive Control. *J. Neurosci.* **27**, 2349–2356 (2007).

43. Seeley, W. W. The Salience Network: A Neural System for Perceiving and Responding to Homeostatic Demands. *J. Neurosci.* **39**, 9878–9882 (2019).

44. Gillan, C. M. *et al.* Disruption in the Balance Between Goal-Directed Behavior and Habit Learning in Obsessive-Compulsive Disorder. *Am. J. Psychiatry* **168**, 718–726 (2011).

45. Silva, C. F. da & Hare, T. A. Humans primarily use model-based inference in the two-stage task. *Nat. Hum. Behav.* **4**, 1053–1066 (2020).

46. Schad, D. J. *et al.* Processing speed enhances model-based over model-free reinforcement learning in the presence of high working memory functioning. *Front. Psychol.* **5**, 1450 (2014).

47. Bickel, W. K. & Marsch, L. A. Toward a behavioral economic understanding of drug dependence: delay discounting processes. *Addiction* **96**, 73–86 (2001).

48. Kozak, K. *et al.* The neurobiology of impulsivity and substance use disorders: implications for treatment. *Ann. N. York Acad. Sci.* **1451**, 71–91 (2019).

49. Poulton, A. & Hester, R. Transition to substance use disorders: impulsivity for reward and learning from reward. *Soc. Cogn. Affect. Neurosci.* **15**, 1182–1191 (2019).

50. Wu, X. *et al.* Functions of Learning Rate in Adaptive Reward Learning. *Front. Hum. Neurosci.* **11**, 592 (2017).

51. Eckstein, M. K. & Collins, A. G. E. Computational evidence for hierarchically structured reinforcement learning in humans. *Proc. Natl. Acad. Sci.* **117**, 29381–29389 (2020).

52. Everitt, B. J. & Robbins, T. W. Drug Addiction: Updating Actions to Habits to Compulsions Ten Years On. *Annu. Rev. Psychol.* **67**, 1–28 (2015).

53. Ostlund, S. B. & Balleine, B. W. On habits and addiction: an associative analysis of compulsive drug seeking. *Drug Discov. Today: Dis. Model.* **5**, 235–245 (2009).

54. Doñamayor, N. *et al.* Goal-Directed and Habitual Control in Human Substance Use: State of the Art and Future Directions. *Neuropsychobiology* **81**, 403–417 (2022).

55. Ersche, K. D. *et al.* Response Perseveration in Stimulant Dependence Is Associated with Striatal Dysfunction and Can Be Ameliorated by a D2/3 Receptor Agonist. *Biol. Psychiatry* **70**, 754–762 (2011).

56. Menon, V. & Uddin, L. Q. Saliency, switching, attention and control: a network model of insula function. *Brain Struct. Funct.* **214**, 655–667 (2010).

57. Uddin, L. Q. Salience processing and insular cortical function and dysfunction. *Nat. Rev. Neurosci.* **16**, 55–61 (2015).

58. Preuschoff, K., Quartz, S. R. & Bossaerts, P. Human Insula Activation Reflects Risk Prediction Errors As Well As Risk. *J. Neurosci.* **28**, 2745–2752 (2008).

59. Jensen, J. *et al.* Separate brain regions code for salience vs. valence during reward prediction in humans. *Hum. Brain Mapp.* **28**, 294–302 (2007).

60. Tolomeo, S. & Yu, R. Brain network dysfunctions in addiction: a meta-analysis of resting-state functional connectivity. *Transl. Psychiatry* **12**, 41 (2022).

61. Hong, S.-B. *et al.* A selective involvement of putamen functional connectivity in youth with internet gaming disorder. *Brain Res.* **1602**, 85–95 (2015).

62. Lee, D., Lee, J., Lee, J. E. & Jung, Y.-C. Altered functional connectivity in default mode network in Internet gaming disorder: Influence of childhood ADHD. *Prog. Neuro-Psychopharmacol. Biol. Psychiatry* **75**, 135–141 (2017).

63. Sun, Y. *et al.* Brain fMRI study of crave induced by cue pictures in online game addicts (male adolescents). *Behav. Brain Res.* **233**, 563–576 (2012).

64. Zheng, H. *et al.* Meta-analyses of the functional neural alterations in subjects with Internet gaming disorder: Similarities and differences across different paradigms. *Prog. Neuro-Psychopharmacol. Biol. Psychiatry* **94**, 109656 (2019).

65. Droutman, V., Read, S. J. & Bechara, A. Revisiting the role of the insula in addiction. *Trends Cogn. Sci.* **19**, 414–420 (2015).

66. Naqvi, N. H., Gaznick, N., Tranel, D. & Bechara, A. The insula: a critical neural substrate for craving and drug seeking under conflict and risk. *Ann. N. York Acad. Sci.* **1316**, 53–70 (2014).

67. Nestor, L., Hester, R. & Garavan, H. Increased ventral striatal BOLD activity during non-drug reward anticipation in cannabis users. *NeuroImage* **49**, 1133–1143 (2010).

68. Stewart, J. L. *et al.* Striatum and insula dysfunction during reinforcement learning differentiates abstinent and relapsed methamphetamine-dependent individuals. *Addiction* **109**, 460–471 (2014).

69. Stewart, J. L. *et al.* You are the danger: Attenuated insula response in methamphetamine users during aversive interoceptive decision-making. *Drug Alcohol Depend.* **142**, 110–119 (2014).

70. Madden, G. J., Petry, N. M., Badger, G. J. & Bickel, W. K. Impulsive and self-control choices in opioid-dependent patients and non-drug-using control patients: Drug and monetary rewards. *Exp. Clin. Psychopharmacol.* **5**, 256–262 (1997).

71. Cushnie, A. K., Tang, W. & Heilbronner, S. R. Connecting Circuits with Networks in Addiction Neuroscience: A Salience Network Perspective. *Int. J. Mol. Sci.* **24**, 9083 (2023).

72. Ko, C.-H. *et al.* Brain activities associated with gaming urge of online gaming addiction. *J. Psychiatr. Res.* **43**, 739–747 (2009).

73. Ko, C.-H. *et al.* The brain activations for both cue-induced gaming urge and smoking craving among subjects comorbid with Internet gaming addiction and nicotine dependence. *J. Psychiatr. Res.* **47**, 486–493 (2013).

74. Turel, O., He, Q., Wei, L. & Bechara, A. The role of the insula in internet gaming disorder. *Addict. Biol.* **26**, e12894 (2021).

75. Gremel, C. M. & Costa, R. M. Orbitofrontal and striatal circuits dynamically encode the shift between goal-directed and habitual actions. *Nat. Commun.* **4**, 2264 (2013).

76. Jones, J. L. *et al.* Orbitofrontal Cortex Supports Behavior and Learning Using Inferred But Not Cached Values. *Science* **338**, 953–956 (2012).

77. Kahnt, T. Computationally Informed Interventions for Targeting Compulsive Behaviors. *Biol. Psychiatry* **93**, 729–738 (2023).

78. McDannald, M. A., Lucantonio, F., Burke, K. A., Niv, Y. & Schoenbaum, G. Ventral Striatum and Orbitofrontal Cortex Are Both Required for Model-Based, But Not Model-Free, Reinforcement Learning. *J. Neurosci.* **31**, 2700–2705 (2011).

79. Howard, J. D., Gottfried, J. A., Tobler, P. N. & Kahnt, T. Identity-specific coding of future rewards in the human orbitofrontal cortex. *Proc. Natl. Acad. Sci.* **112**, 5195–5200 (2015).

80. Lopatina, N. *et al.* Lateral orbitofrontal neurons acquire responses to upshifted, downshifted, or blocked cues during unblocking. *eLife* **4**, e11299 (2015).

81. Boisgueheneuc, F. du *et al.* Functions of the left superior frontal gyrus in humans: a lesion study. *Brain* **129**, 3315–3328 (2006).

82. Dom, G., Sabbe, B., Hulstijn, W. & Brink, W. van D. Substance use disorders and the orbitofrontal cortex. *Br. J. Psychiatry* **187**, 209–220 (2005).

83. Moorman, D. E. The role of the orbitofrontal cortex in alcohol use, abuse, and dependence. *Prog. Neuro-Psychopharmacol. Biol. Psychiatry* **87**, 85–107 (2018).

84. López-Caneda, E. *et al.* Hyperactivation of right inferior frontal cortex in young binge drinkers during response inhibition: a follow-up study. *Addiction* **107**, 1796–1808 (2012).

85. Grant, J. E., Potenza, M. N., Weinstein, A. & Gorelick, D. A. Introduction to Behavioral Addictions. *Am. J. Drug Alcohol Abus.* **36**, 233–241 (2010).

86. Han, J. W. *et al.* Differences in functional connectivity between alcohol dependence and internet gaming disorder. *Addict. Behav.* **41**, 12–19 (2015).

87. Oscar-Berman, M. & Marinković, K. Alcohol: Effects on Neurobehavioral Functions and the Brain. *Neuropsychol. Rev.* **17**, 239–257 (2007).

88. Weinstein, A. & Lejoyeux, M. Neurobiological mechanisms underlying internet gaming disorder. *Dialogues Clin. Neurosci.* **22**, 113–126 (2020).

89. Friston, K. J., Zarahn, E., Josephs, O., Henson, R. N. A. & Dale, A. M. Stochastic Designs in Event-Related fMRI. *NeuroImage* **10**, 607–619 (1999).

Appendix

Table S1. Linear mixed-effects logistic regression results for stay probability

	HC		IGD		AUD	
	Coef [95% CI]	*p* value	*Coef* [95% CI]	*p* value	*Coef* [95% CI]	*p* value
Reward	-0.778 [-1.129, -0.427]	*p*=1.40e-05	-1.117 [-1.440, -0.794]	*p*=1.19e-11	-1.119 [-1.536, -0.702]	*p*=1.44e-07
Transition probability	-1.077 [-1.406, -0.748]	*p*=1.40e-10	-1.055 [-1.374, -0.735]	*p*=9.38e-11	-1.238 [-1.954, -0.523]	*p*=0.001
Reward x transition probability	1.970 [1.661, 2.279]	*p*<2.00e-16	3.311 [2.912, 3.709]	*p*<2.00e-16	3.204 [-2.776, 3.631]	*p*<2.00e-16

The table reports the coefficients, 95% confidence intervals (CIs), and p-values for the main effects of reward, transition probability, and the interaction. The residual degree of freedom for each group are as follows: HC = 5,969, IGD = 4,370, AUD = 4,385[30] .

Table S2. Second-level results of model-based fMRI analysis

Group	Corresponding Brain Region	Peak MNI Coordinates (x, y, z)	T value	Z value	*p* value (peak voxel)	*p* value (cluster level)	cluster size
HC	Fusiform gyrus (L)	-36, -84, -8	4.82	4.01	$p < 0.001^{*}$	$p = 0.102$	10
IGD	Insula (R)	42, 14, -14	4.56	3.64	$p < 0.001^{*}$	$p = 0.085$	15
AUD	Orbitofrontal cortex (R)	35, 55, -8	6.39	4.56	$p < 0.001^{*}$	$p = 0.016^{\dagger}$	29
	Occipital lobe (R)	31, -91, -4	5.15	3.98	$p < 0.001^{*}$	$p = 0.088$	13
	Posterior cingulate cortex	1, -35, 36	5.05	3.93	$p < 0.001^{*}$	$p = 0.013^{\dagger}$	31
	Occipital lobe (L)	-22, -99, -4	4.98	3.90	$p < 0.001^{*}$	$p = 0.088$	13
	Anterior cingulate cortex	-3, 44, 6	4.91	3.86	$p < 0.001^{*}$	$p = 0.019^{\dagger}$	27

The table presents the significant findings from second-level one-sample t-tests performed as part of the model-based fMRI analysis, incorporating the model-based reward prediction error (RPE) as a parametric modulator ($p < 0.001$, uncorrected; cluster size, $k \geq 10$). Asterisks (*) denote results significant at $p < 0.001$, while cross symbols (†) indicate significance at $p < 0.05$[30] .

Table S3. PPI second-level results for the internet gaming disorder (IGD) group

Seed region	Corresponding Brain Region	Peak MNI Coordinates (x, y, z)	T value	Z value	*p* value (uncorrected)	*p* value (cluster level)	cluster size
Insula (R)	Putamen (R)	31, 2, -14	5.23	3.98	$p < 0.001^{*}$	$p = 0.014^{\dagger}$	24
	Insula (L)	-48, 10, -8	5.75	4.23	$p < 0.001^{*}$	$p = 0.346$	3
	Occipital lobe	-48, -76, -4	4.37	3.53	$p < 0.001^{*}$	$p = 0.601$	1
		46, -72, -4	4.31	3.50	$p < 0.001^{*}$	$p = 0.110$	9
		-48, -69, 6	4.23	3.45	$p < 0.001^{*}$	$p = 0.445$	2
Insula (L)	Anterior Cingulate Cortex	5, 10, 32	4.24	3.45	$p < 0.001^{*}$	$p = 0.012^{\dagger}$	24
	Superior temporal gyrus (R)	31, -9, -4	3.67	3.11	$p = 0.001^{\dagger}$	$p = 0.587$	1
	Occipital lobe	38, -50, -18	5.14	3.94	$p < 0.001^{*}$	$p = 0.119$	8
		-40, -69, -14	4.82	3.78	$p < 0.001^{*}$	$p = 0.330$	3
		-36, -88, -4	3.92	3.27	$p = 0.001^{\dagger}$	$p = 0.429$	2
		-40, -58, -14	3.89	3.24	$p = 0.001^{\dagger}$	$p = 0.429$	2
		8, -84, -4	3.82	3.2	$p = 0.001^{\dagger}$	$p = 0.429$	2
		-40, -80, -8	3.72	3.14	$p = 0.001^{\dagger}$	$p = 0.587$	1

The table summarizes the significant findings from psychophysiological interaction (PPI) analysis conducted at the second-level one-sample t-tests conducted for the IGD group, with the model-based reward prediction error (RPE) serving as the psychological variable ($p < 0.001$, uncorrected; cluster size, $k \geq 10$). After applying small volume correction using an extent brain mask derived from meta-analytic brain maps of "salience", "salience network", and "reward" extracted from the Neurosynth, the resulting clusters within the corrected volume were smaller than the initially applied threshold of $k \geq 10$. Asterisks (*) denote results significant at $p < 0.001$, and cross symbols (†) indicate significance at $p < 0.05$[30] .

Table S4. Second-level group comparison results of the PPI analysis

Group	Seed region	Corresponding Brain Region	Peak MNI Coordinates (x, y, z)	T value	Z value	*p* value (uncorrected)	*p* value (cluster level)	cluster size
Insula (R)	HC < IGD	Insula (L)	-48, 10, -8	3.89	3.59	$p < 0.001^{*}$	$p = 0.513$	2
		Parietal frontal lobe (R)	35, 6, 56	3.61	3.36	$p < 0.001^{*}$	$p = 0.292$	5
		Premotor cortex (R)	27, -5, 52	3.31	3.11	$p < 0.001^{*}$	$p = 0.657$	1
		Fusiform gyrus (R)	46, -54, -18	3.75	3.47	$p < 0.001^{*}$	$p = 0.657$	1
			31, -61, -18	3.34	3.14	$p < 0.001^{*}$	$p = 0.657$	1
		Parietal lobe (R)	46, -31, 42	3.66	3.4	$p < 0.001^{*}$	$p = 0.657$	1
		Occipital lobe	31, -84, -8	3.67	3.41	$p < 0.001^{*}$	$p = 0.347$	4
			5, -69, 46	3.55	3.31	$p < 0.001^{*}$	$p = 0.513$	2
			-40, -58, -18	3.54	3.31	$p < 0.001^{*}$	$p = 0.417$	3
			-14, -72, 52	3.54	3.31	$p < 0.001^{*}$	$p = 0.657$	1
			12, -84, 6	3.51	3.28	$p < 0.001^{*}$	$p = 0.513$	2
			-6, -84, -4	3.44	3.22	$p < 0.001^{*}$	$p = 0.513$	2
	AUD < IGD	Occipital lobe	-10, -95, -4	4.41	3.92	$p < 0.001^{*}$	$p = 0.083$	13
			12, -84, 2	4.09	3.69	$p < 0.001^{*}$	$p = 0.392$	3
			-25, -95, 6	3.57	3.29	$p < 0.001^{*}$	$p = 0.637$	1
			31, -95, -4	3.52	3.25	$p < 0.001^{*}$	$p = 0.321$	4
Insula (L)	AUD < IGD	Occipital lobe	12, -95, 12	3.79	3.46	$p < 0.001^{*}$	$p = 0.492$	2
			-25, -95, 6	3.41	3.16	$p < 0.001^{*}$	$p = 0.639$	1
	AUD > IGD	Posterior cingulate cortex	-3, -46, 32	3.81	3.47	$p < 0.001^{*}$	$p = 0.271$	5

The table presents the findings from second-level group comparisons conducted using two-sample t-tests in the psychophysiological interaction (PPI) analysis ($p < 0.001$, uncorrected; cluster size, $k \geq 10$). Following small volume correction with an extent brain mask derived from meta-analytic brain maps of "salience", "salience network", and "reward" extracted from the Neurosynth, the resulting clusters within the corrected volume were smaller than the initially applied threshold of $k \geq 10$. Asterisks (*) denote results significant at $p < 0.001$, and cross symbols (†) indicate significance at $p < 0.05$[30] .

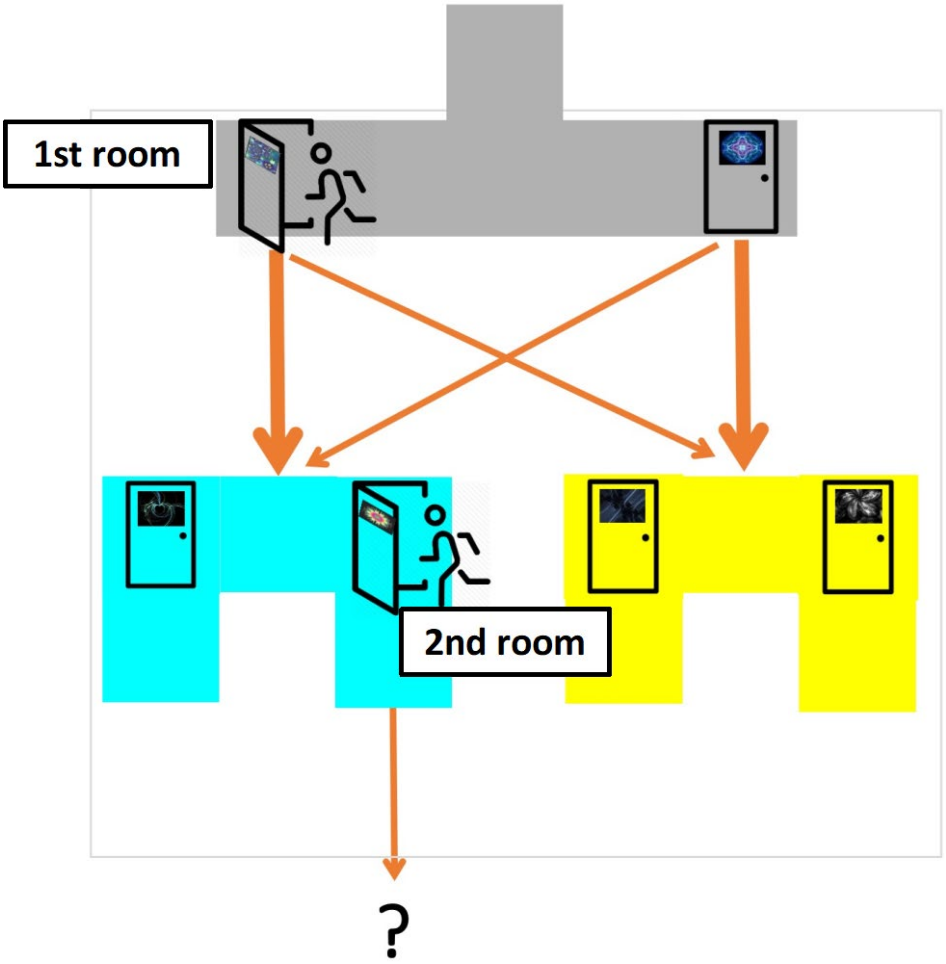

Figure S1. Schematic representation of the two-stage task used in instructions. This figure illustrates an example of the two-stage task as presented in the task instructions. The schematic includes a depiction of exemplary choices, with a human icon representing the choices available at each stage[30] .

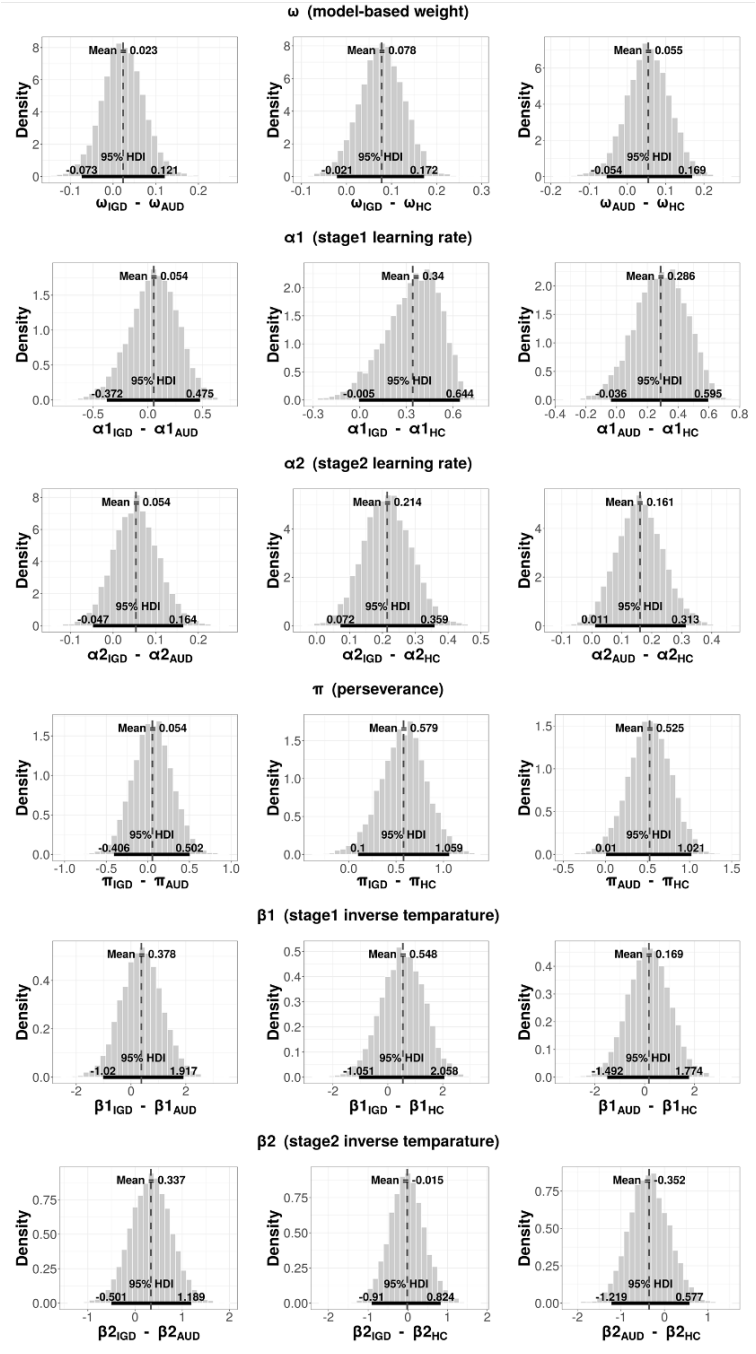

Figure S2. **Distribution of group differences in model parameter estimates.** This figure shows the

distributions of group differences in model parameter estimates, calculated for each pairwise comparison (IGD vs. AUD; IGD vs. HC; AUD vs. HC). The distributions represent the subtracted values of one group's parameter estimates from another's (e.g., ω_IGD-ω_AUD). Black lines beneath the distributions indicate the 95% highest density interval (HDI). Group differences are considered significant if the 95% HDI does not include zero[30] .

Abstract in Korean

인터넷 게임장애의 모델기반 및 모델프리 강화학습에 관여하는 신경상관체

연구 배경 및 목적: 인터넷 게임 장애(Internet gaming disorder, IGD)는 심각한 공중보건 문제가 되었으나, 그 신경인지 메커니즘은 아직 명확하지 않다. 따라서, IGD와 알코올 사용 장애(AUD)를 비롯한 다른 중독성 장애들과의 유사점과 차이점을 파악하는 것은 중요한 문제이다. 최근의 연구들은, 계산 심리학적 접근과 의사 결정 프레임워크가 IGD를 개념화하고 정신과 질환과의 유사성과 차이점을 구분하는데 유리하다는 것을 지지하고 있다. 본 연구에서는 IGD와 AUD 환자에서 목표지향적(모델기반) 및 습관성(모델프리) 조절 시스템과 관련된 신경인지적 특성을 규명하고자 하였다.

연구 재료 및 방법: 젊은 남성들 중 IGD (n=24), AUD (n=22), 그리고 건강한 대조군 (HC; n=30)으로 진단된 피험자들은 two-stage task를 수행하면서 fMRI검사를 시행 받았다. Two-stage task는 모델기반 및 모델프리 조절 시스템으로부터의 기여도를 평가하기 위해 검증된 과제이다. 본 연구의 목적은, 계산 모델링과 계층 베이지안 분석을 사용하여 IGD, AUD, 그리고 HC 그룹의 두 의사결정 시스템(모델 기반/모델 프리 학습) 간의 균형을 조사하는 것이다. 마지막으로, 우리는 모델 기반 fMRI 분석을 통해 IGD와 AUD의 목표지향적 조절과 관련한 신경상관체를 도출해내고자 하였다.

연구 결과: 계산 모델링 결과, IGD와 AUD 그룹 모두 유사한 수준의 모델 기반 행동을 보였다. 그러나 두 그룹 간에 모델 기반 보상 예측 오류(RPE)에 대한 신경상관체는 구별되는 차이가 있었다. IGD 그룹은 모델 기반 RPE와 관련하여

섬엽에서 활성화를 보인 반면, AUD 그룹은 전두엽 영역, 특히 안와전두 피질과 상부 전두회에서 활성화를 보였다. 또한, IGD 그룹은 모델 기반 RPE의 기능적 연결성 관점에서 섬엽과 현저성 네트워크(salience network)과 관련된 뇌영역들 간의 과다 연결성을 나타냈다.

결론: 본 연구는 IGD와 AUD가 계산 모델링에서 나타나는 공통된 인지적 특성에도 불구하고, IGD와 AUD에서 모델 기반 행동을 매개하는 신경생물학적 메커니즘이 다를 수 있음을 시사한다. 본 연구는 모델 기반 시스템과 관련하여 IGD와 AUD를 비교한 첫 번째 신경영상 연구로서, IGD만의 특징적인 의사결정 과정을 이해하는 데 새로운 관점을 제공한다.

핵심되는 말 : 인터넷 게임장애, 알코올 사용장애, 목표지향적 조절, 모델 기반 fMRI